Received January 15, 2019, accepted February 5, 2019, date of publication February 21, 2019, date of current version April 16, 2019.

Digital Object Identifier 10.1109/ACCESS.2019.2900517

Acceleration for HEVC Encoder by Bimodal Segmentation of Rate-Distortion Cost and Accurate Determination of Early Termination and Early Split

KUANG-HAN TAI[1], MEI-JUAN CHEN[1], (Senior Member, IEEE), JIE-RU LIN[1], (Student Member, IEEE), REN-YUAN HUANG[1], CHIA-HUNG YEH[2,3], (Senior Member, IEEE), CHIA-YEN CHEN[4], (Member, IEEE), SHINFENG D. LIN[5], (Senior Member, IEEE), RO-MIN WENG[1], (Member, IEEE), AND CHUAN-YU CHANG[6], (Senior Member, IEEE)

[1]Department of Electrical Engineering, National Dong Hwa University, Hualien, Taiwan
[2]Department of Electrical Engineering, National Taiwan Normal University, Taipei, Taiwan
[3]Department of Electrical Engineering, National Sun Yat-sen University, Kaohsiung, Taiwan
[4]Department of Computer Science, The University of Auckland, Auckland, New Zealand
[5]Department of Computer Science and Information Engineering, National Dong Hwa University, Hualien, Taiwan
[6]Department of Computer Science and Information Engineering, National Yunlin University of Science and Technology, Yunlin, Taiwan

Corresponding author: Chia-Hung Yeh (chyeh@ntnu.edu.tw)

This work was supported in part by the Ministry of Science and Technology, Taiwan, under Grant NSC 102-2221-E-259-022-MY3 and Grant MOST 105-2221-E-259-016-MY3, and in part by the "Intelligent Recognition Industry Service Center" from the Featured Areas Research Center Program within the framework of the Higher Education Sprout Project by the Ministry of Education (MoE), Taiwan.

ABSTRACT The processing unit with a quad-tree structure in high efficiency video coding (HEVC/H.265) consists of a coding unit (CU), a prediction unit (PU), and a transform unit (TU). The CU and PU account for the majority of the computational complexity. This paper proposes a fast inter-prediction algorithm to overcome the high-computational demand associated with the coding complexity for an HEVC/H.265 encoder. In this paper, the CU depth prediction is proposed to reduce the number of CU executions by incorporating the depths and rate-distortion costs (RD-costs) of the adjacent CUs. Bimodal RD-cost segmentation is proposed for the elementary dichotomy of RD-cost distribution. The proposed algorithm applies the one-sided Chebyshev's inequality for the determination of accurate RD-cost thresholds by adjusting the error rates for early termination and early split. Our approach achieves 50.1% and 48.7% time savings with Bjøntegaard delta bit rate (BDBR) increases of 1.2% and 1.0% compared to the HEVC/H.265 reference software for random access and low delay configurations, respectively. The proposed method has better performance than earlier researches in terms of both coding speed and rate-distortion.

INDEX TERMS High efficiency video coding, HEVC, H.265, bimodal segmentation, RD-cost, one-sided Chebyshev's inequality, early termination, early split.

I. INTRODUCTION

Video applications have become widely popular and the re solution of video is continually increasing. Thanks to the fast transmission capability of the Internet, real-time video streaming is becoming more useful than ever. The quality and resolution requirements of multimedia applications are rising dramatically along with bandwidth growing up [1]–[3]. Nowadays, ultra-high definition TV (UHDTV) supports 8K × 4K resolution, and 4K (3840 × 2160) smartphones have recently become available on the market. An 8K UHDTV (7680 × 4320, 4320p, 4:2:0, 30fps) video signal requires 11391 Mbps of bitrate and about 1423 MB for one second of video. When it comes to state-of-the-art quadruple-layered (BD-XL, 128 GB) Blu-ray Disks, one disk is capable of holding only 92 seconds of raw 8K UHD video data. Real-time

The associate editor coordinating the review of this manuscript and approving it for publication was Zhaoqing Pan.

transmission of the aforementioned video data is beyond the capabilities of contemporary networks. In order to handle this prohibitively high video signal bitrate, developing efficient video compression technique is necessary.

The newest international video coding standard High Efficiency Video Coding (HEVC/H.265) [4] has been improved nearly twofold compared to the previous video standard, Advanced Video Coding (H.264/AVC) [5]. Compared to H.264/AVC, which is widely applied to high definition (HD) video signals, HEVC/H.265 can efficiently encode the videos beyond HD resolution (e.g., 4K and 8K ultra-high-definition resolutions). However, the coding complexity of HEVC/H.265 is much higher than that of previous standards. Thus, devising a way to reduce the coding complexity of the HEVC/H.265 encoder, thereby making it more conducive to use in practical applications is the purpose of this paper.

II. RELATED WORKS

HEVC/H.265 achieves significantly improved compression efficiency by taking advantage of novel compression methods. Nevertheless, it brings the disadvantage of huge of computation. Researchers have proposed efficient algorithms to reduce the HEVC encoder's computational complexity [6]. CU is not split in [7] if the SKIP mode is employed. Early SKIP detection [8] checks inter $2N \times 2N$ first and ignores other PU modes if SKIP is selected. Coding Flag Mode (CFM) [9] is designed for terminating the PU mode decision when the coded block flag (CBF) is active for the current PU. However, the bitrate rises when the encoding time is reduced.

A hierarchical complexity control approach in [10] accurately reduces the coding complexity to the target bandwidth and keeps video quality simultaneously. Reference [11] proposes a rate control scheme for region of interest (ROI) based on Fourier transform and neuron network. Reference [12] proposes an early SKIP mode decision, utilizing the characteristics of the SKIP mode to reduce the complexity. If the best prediction mode in the current CU depth and those of the reference CUs are SKIP mode, the procedure of the encoding CU can be terminated. Kim *et al.* [13] propose a method to check PU of type $2N \times 2N$ first; then checks its CBF and the motion vector difference (MVD) to decide if skip early or not. If these two values are zero, the rest of the PU types in the current CU depth are ignored and the next CU depth can be checked directly. Reference [14] applies a threshold attained by reference to average SKIP mode RD-cost and checks CBF to skip PUs. Reference [15] defines that if the sum of the RD costs of the current depth CU is larger than the RD cost of its parent CU, the CU procedure is terminated. In addition, the average RD cost of previously coded SKIP modes is computed as a threshold. If the RD cost of the current CU is smaller than the threshold, there is no need to further split the CU. In [16], if the average of the RD cost of the SKIP mode coded before multiplied by a weighting factor is larger than the RD cost of the current CU's SKIP mode, then CU early termination is triggered. In addition, if the sum of the RD costs of the current depth CU is larger than the RD cost of its parent CU, the CU procedure is terminated. The works in [17] and [18] present a CU selection algorithm according to motion homogeneity, and apply spatio-temporal correlation of CU depth to predict which depth level should be checked. In [19] and [20], a threshold is set based on the best prediction mode's RD-cost of spatio-temporal CUs to cut mode candidates. In [21], skip estimation and early termination for CU size decision are proposed to diminish HEVC/H.265 encoder's computations. In [22], the encoding procedure is accelerated both at the levels of frame and coding unit. In the frame level algorithm, the ratio of the number of CUs in the current depth in the previous frame to the number of CUs in the next depth in the previous frame is computed. If the ratio is smaller than or equal to a threshold, the current depth can be skipped. Conversely, if the ratio is greater than a threshold, all the PU types in the current CU will be performed completely. In the CU level, if the depths of the neighboring CUs are greater than the current depth, it is not necessary to further split them.

Reference [23] adaptively selects the CU depth range for effective splitting. Reference [24] reduces the coding complexity by dynamically adjusting CU depth and compares the results under various constrained complexity reduction ratios. In [25], a complexity allocation scheme is proposed by linear programming to maximize the RD-performance. In addition, a flexible mode selection is designed according to allocated complexity factor. Reference [26] analyzes the RD-complexity of different inter modes and the execution of symmetric motion partition (SMP) and asymmetric motion partition (AMP) is determined to accelerate the prediction. Reference [27] analyzes the relation of motion compensation cost and the sum of absolute differences (SAD) cost for fast deciding CU. Reference [28] trains the decision trees by using data mining tool and the computation complexities of CU, PU, and RQT(residual quadtree) are decreased. In [29], the distributions of distortion and residual are utilized to decide whether to skip PU modes and motion estimation (ME). In [30], the inter modes and spatio-temporal correlation are analyzed by Transparent Composite Model (TCM) and a fast inter mode decision method is proposed. Reference [31] proposes a complexity control method combined with the early termination conditions, which the thresholds of the early termination conditions are dynamically attuned.

Reference [32] proposes a data driven algorithm based on data training and classification to effectively decide the CU sizes for intra coding. Reference [33] incorporates the correlations of inter-level and spatio-temporal to speedup the encoder process. In [34], Edge Offset of Sample Adaptive Offset (SAO) of the neighboring CTUs is used to early decide SKIP mode. Reference [35] formulates the time-consuming CU splitting process as a cascaded classification task and reduces the coding time by based on fuzzy support vector machine (SVM). In [36], the multiple reference frames (MRF) during inter prediction are early selected and optimized based on content similarity to reduce the computational complexity. Reference [37] proposes an early skip detection by identifying the motionless and homogeneous regions. Reference [38] acquires edge information within a CTU and conceives a fast mode decision method according to the edge diversities.

This paper proposes an inter-prediction algorithm by early termination and early split of the procedures of coding unit and prediction unit. Our approach investigates the trade-off between the RD performance and coding speed and provides better performance than previous works.

III. PROPOSED ALGORITHM

Inter-prediction in HEVC/H.265 encoder performs mode decision and ME for all the PU types for every CU depth, and thus also incurs a massive computational burden. In the proposed algorithm, adaptive CU depth estimation is designed to eliminate irrelative depths. Bimodal RD-cost segmentation is implemented by Otsu's automation segmentation for elementary dichotomy of RD-cost. One-sided Chebyshev's theorem is applied to control the error rate to ensure accurate early termination and early split. Adaptive search range is also adopted in our scheme.

A. ADAPTIVE CU DEPTH ESTIMATION ALGORITHM

In order to accelerate the CU depth estimation procedure, we obtain the minimum depth ($Depth_{LBound}$) and maximum depth ($Depth_{UBound}$) values of reference CTUs of the current CTU as shown in (1) and (2). Fig. 1 visualizes the neighboring CTUs, which are used to obtain $Depth_{LBound}$ and $Depth_{UBound}$.

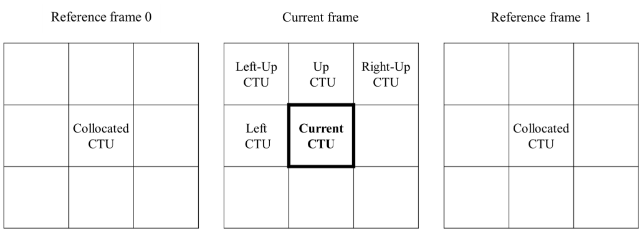

FIGURE 1. Illustration of neighbor CTUs in proposed inter-prediction algorithm.

Moreover, the predicted depth ($Depth_{pre}$) is determined by the information of the depths incorporated with the RD-costs in all neighboring CUs. The predicted depth for the current CU is the weighted sum, which is calculated by the inverse of RD-costs and the depth of neighboring CUs plus one, as indicated in (3) as our previous work [39] for intra-prediction. The total weighted sum, calculated by the inverse of RD-costs, is shown in (4). The i or j means the index of neighboring CUs. The n indicates the number of CUs within neighboring CTUs. $Depth_i$ and $RDcost_i$ indicate the depth and the corresponding RD-cost of the i-th neighboring CUs, respectively. The smaller the RD-cost of neighboring CUs, the more significant this is for the corresponding depth. In order to avoid a zero value for depth 0, one is added to $Depth_i$ to get the $Depth_{pre}$.

$$Depth_{LBound} = \min Depth_{CU}, \quad CU \in CTU_{Neighbor} \tag{1}$$

$$Depth_{UBound} = \max Depth_{CU}, \quad CU \in CTU_{Neighbor} \tag{2}$$

$$Depth_{pre} = truncate\Big(\frac{1}{Weight_{Total}}\sum_{i=0}^{n-1}\Big(\frac{1}{RDcost_i \times 4^{Depth_i}} \times (Depth_i + 1)\Big)\Big) \tag{3}$$

$$Weight_{Total} = \sum_{j=0}^{n-1}\frac{1}{RDcost_j \times 4^{Depth_j}} \tag{4}$$

$$Depth_{LBound} = Depth_{LBound} - 1, \quad if\ Depth_{pre} == Depth_{LBound} \tag{5}$$

$$Depth_{UBound} = Depth_{UBound} + 1, \quad if\ Depth_{pre} == Depth_{UBound} \tag{6}$$

$$Depth_{LBound} = max\{Depth_{LBound}, 0 \tag{7}$$

$$Depth_{UBound} = min\{Depth_{UBound}, 3\} \tag{8}$$

Although early splitting and early terminating CU methods speed up the CU and bypass the PU and TU processes, this improvement is accompanied by RD performance degradation. To mitigate this drawback, we jointly consider the $Depth_{pre}$ with $Depth_{LBound}$ and $Depth_{UBound}$. When $Depth_{pre}$ is equal to $Depth_{LBound}$, it means the predicted depth is close to the predicted lower bounded depth. The $Depth_{LBound}$ has one subtracted from it to maintain the coding performance, as specified in (5). On the other hand, one is added to $Depth_{UBound}$ when $Depth_{pre}$ equals $Depth_{UBound}$, as shown in (6). Equations (7) and (8) constrain $Depth_{LBound}$ and $Depth_{UBound}$ within CU depth 0 to 3.

To verify the capability of the proposed depth estimation algorithm, we investigate the accuracies of the individual neighboring CU depth and the proposed algorithm ($Depth_{LBound}$, $Depth_{UBound}$, and $Depth_{pre}$). As listed in TABLE 1, the simulation includes 25 testing sequences (Class A-F) for random access configuration with quantization parameters (QP) of 22, 27, 32 and 37. The depth of the reference CUs (Left, Up, Left-Up, Right-Up and Collocated) are predicted correctly if the depth of reference CU is equal to the actual depth of current CU. $Depth_{LBound}$ is predicted correctly if the actual depth of current CU is larger than or equal to $Depth_{LBound}$. $Depth_{UBound}$ is predicted correctly if the actual depth of current CU is smaller than or equal to $Depth_{UBound}$. The $Depth_{pre}$ is predicted correctly if $Depth_{pre}$ is equal to the actual depth of current CU. TABLE 2 shows the average probabilities of the accuracies for individual neighboring CU depth and the proposed algorithm. As can be seen from TABLE 2, the collocated CUs obtain the highest probability among the reference CUs, followed, in descending order, by Left CU, Up CU, Right-Up CU and Left-Up CU. In terms of the $Depth_{LBound}$ and $Depth_{UBound}$, the probabilities are more than 99%. The probability of $Depth_{pre}$ is

TABLE 1. Testing sequences for simulation.

Class	Name		Resolution	Frames	Fps
A	S01	Traffic	2560 × 1600	150	30
A	S02	PeopleOnStreet	2560 × 1600	150	30
B	S03	Kimono	1920 × 1080	240	24
B	S04	ParkScene	1920 × 1080	240	24
B	S05	Cactus	1920 × 1080	500	50
B	S06	BasketballDrive	1920 × 1080	500	50
B	S07	BQTerrace	1920 × 1080	600	60
C	S08	BasketballDrill	832 × 480	500	50
C	S09	BQMall	832 × 480	600	60
C	S10	PartyScene	832 × 480	500	50
C	S11	RaceHorses	832 × 480	300	30
D	S12	BasketballPass	416 × 240	500	50
D	S13	BQSquare	416 × 240	600	60
D	S14	BlowingBubbles	416 × 240	500	50
D	S15	RaceHorses	416 × 240	300	30
E	S16	Vidyo1	1280 x 720	600	60
E	S17	Vidyo3	1280 x 720	600	60
E	S18	Vidyo4	1280 x 720	600	60
E		FourPeople	1280 × 720	600	60
E		Johnny	1280 × 720	600	60
E		KristenAndSara	1280 × 720	600	60
F	S23	BasketballDrillText	832 x 480	500	50
F	S24	ChinaSpeed	1024 x 768	500	30
F	S25	SlideEditing	1280 x 720	300	30
F	S26	SlideShow	1280 x 720	500	20

TABLE 2. Accuracy(%) of CU depth estimation.

Sequence		Left	Left-Up	Up	Right-Up	Collocated	$Depth_{LBound}$	$Depth_{UBound}$	$Depth_{pre}$
A	S01	82.78	76.55	80.58	78.75	89.10	99.88	99.55	92.40
A	S02	87.38	82.83	86.00	82.98	92.20	99.90	99.50	92.40
B	S03	62.85	57.50	60.85	56.33	64.30	100.00	98.05	68.80
B	S04	78.95	70.55	76.75	69.60	87.00	99.90	99.35	91.50
B	S05	82.15	75.83	80.55	76.10	88.30	99.88	99.33	95.20
B	S06	75.10	63.90	68.78	64.18	75.10	100.00	99.00	89.90
B	S07	83.60	70.40	75.25	73.50	83.00	99.88	98.68	87.40
C	S08	87.55	75.70	82.23	75.88	98.30	99.98	100.00	99.90
C	S09	81.48	68.85	79.63	71.38	91.60	99.60	98.73	95.10
C	S10	91.73	80.20	87.18	80.30	99.40	99.95	100.00	99.50
C	S11	80.58	69.55	78.73	69.50	90.70	99.80	99.68	96.90
D	S12	74.30	49.35	65.55	45.75	82.40	99.93	99.35	97.80
D	S13	86.13	63.90	73.85	52.60	99.40	99.73	100.00	99.70
D	S14	87.00	64.15	75.80	53.98	99.30	99.80	99.98	99.80
D	S15	84.38	62.18	74.68	54.58	96.70	99.93	99.95	98.80
E	S16	76.20	66.88	73.60	67.83	81.60	99.88	98.83	94.00
E	S17	74.50	63.78	71.70	65.48	77.20	99.65	98.25	86.20
E	S18	70.45	63.00	69.13	64.48	75.50	99.43	98.20	85.40
E	Four	81.35	73.10	79.58	73.00	88.40	100.00	99.08	92.70
E	Johnny	72.35	65.65	74.40	65.98	70.20	99.98	98.48	77.60
E	Kristen	70.60	64.58	73.20	64.45	73.60	99.93	99.00	84.10
F	S23	88.10	76.05	83.08	76.93	98.50	99.98	100.00	99.90
F	S24	76.68	56.33	62.35	55.90	72.80	99.38	98.50	89.30
F	S25	79.68	64.23	73.80	64.60	83.20	99.90	99.30	92.20
F	S26	80.73	63.35	67.08	62.00	70.80	99.95	97.15	81.40
Average		79.86	67.54	74.97	66.64	85.14	99.85	99.12	91.52

91.52%. TABLE 2 indicates that the proposed depth estimation algorithm is effective.

B. BIMODAL RD-COST SEGMENTATION BY OTSU'S ALGORITHM

By analyzing the RD-costs of the final best CUs (Non-split CU) and the RD-costs of CUs to be further split (Split CU), we intend to explore a suitable method of early termination and early split. Fig. 2, Fig. 3, and Fig. 4 indicate the probability distributions of rate distortion costs at depth 0, 1, 2 with QP 22, 27, 32, and 37 for Non-split and Split CUs for the S14 sequence. In these figures, the vertical-axis represents the probability of Non-split and Split RD-costs, while the horizontal-axis represents the RD-cost for Non-split CUs and Split CUs, which are collected in each CU depth from the pruning process of the original HM. The blue curve represents the distribution of the RD-costs of Non-split

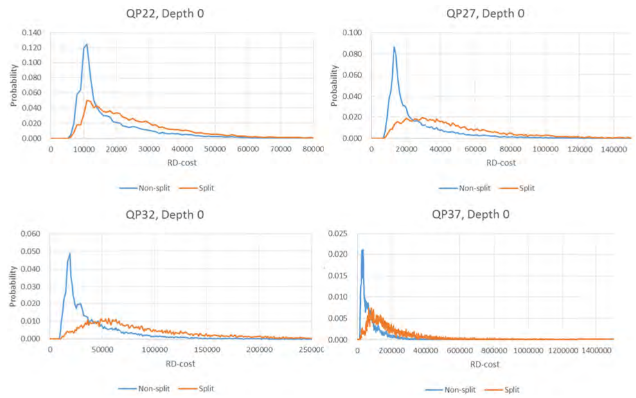

FIGURE 2. Probability distributions of RD-costs at depth 0 with QP 22, 27, 32, and 37 for split and non-split CUs for the S14 sequence.

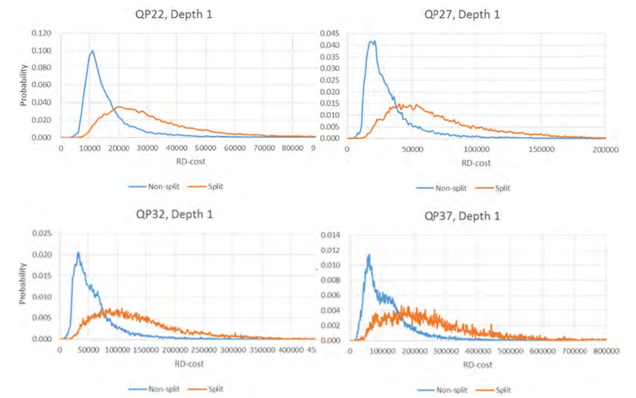

FIGURE 3. Probability distributions of RD-costs at depth 1 with QP 22, 27, 32, and 37 for split and non-split CUs for the S14 sequence.

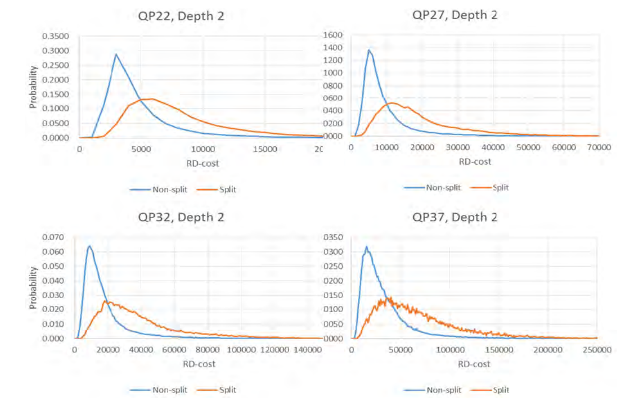

FIGURE 4. Probability distributions of RD-costs at depth 2 with QP 22, 27, 32, and 37 for split and non-split CUs for the S14 sequence.

CUs, and these come from the final CU. On the other hand, the orange curve shows the distributions of the RD-costs of Split CUs, and these come from the CU to be further split. The RD-costs of Non-split CUs tend to be small, and the distribution is concentrated. In contrast, the RD-costs of Split CUs tend to be large, and the distribution is divergent. The curves corresponding to various QPs with the same depth are quite similar, and the curves corresponding to the same QP with various depths are also similar.

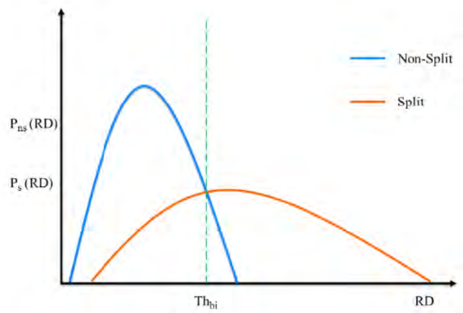

FIGURE 5. **Illustration of the Th_{bi} threshold.**

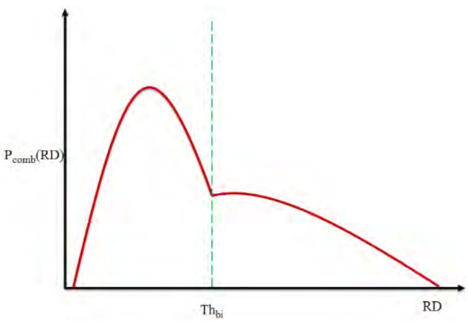

FIGURE 6. **Illustration of combined probability for selecting the Th_{bi} threshold.**

According to this trend, we try to figure out a suitable threshold (Th_{bi}) for early termination and early split to speed up the encoder as shown in Fig. 5. In this paper, we apply Otsu's automatic thresholding [40] to find the threshold Th_{bi} for the combined probability of Non-split CU and Split CU as indicated in Fig. 6. The combined probability is obtained by picking the maximum value for each RD-cost from the probabilities of Non-split CU and Split CU in Fig. 5.

Otsu's automatic thresholding is a threshold selection mechanism and is not only suitable for applications relating to image binarization. As long as the threshold selection is automatic, it can be applied to various practical problems. In this paper, we explore a suitable threshold to separate two classes of RD-costs in Fig. 6 for early termination and early split by applying Otsu's thresholding algorithm for the combined probability. The algorithm calculates through all the possible threshold values, so that the threshold value separates the two classes of RD-costs, such that the variance within classes is minimal and the variance between classes is maximal.

C. ACCURATE RD-COST THRESHOLDS OF EARLY TERMINATION AND EARLY SPLIT BY ERROR RATE ADJUSTMENT

In the above subsection, we propose a bimodal RD-cost segmentation method to obtain a threshold in order to accelerate the encoding process. However, applying the dichotomy threshold to early terminate or early split CU coding process is too rough and might cause significant RD performance degradation.

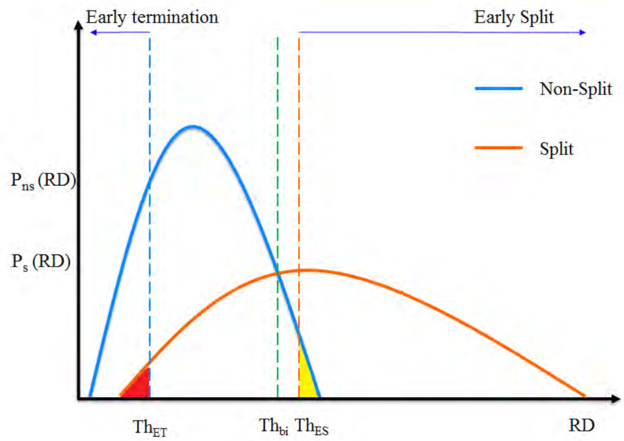

FIGURE 7. **Illustration of the Th_{ET}, Th_{bi} and Th_{ES} thresholds.**

In order to specifically overcome the aforementioned disadvantage, we adjust the RD-cost thresholds by accurately controlling the error rate. As shown in Fig. 7, the error rate means that the CU coding process is determined to be early terminated yet it should be split (red area) continuously, On the other hand, the CU coding process is determined to be early split yet it should be terminated (yellow area) continuously. The RD-cost of the Non-Split CU means that the value of the RD-cost comes from each CU depth and it belongs to the best CU depth finally. On the other hand, the RD-cost of the Split CU means that the value of the RD-cost comes from each CU depth, and it does not belong to the best CU depth in the end. We use these two classes of RD-costs to obtain a threshold for early termination (Th_{ET}) and a threshold for early split (Th_{ES}) by applying one-sided Chebyshev's inequality [41] to speedup the CU coding process, as shown in Fig. 7.

In probability theory, Chebyshev's inequality indicates that almost all random variables are close to the average, and is applied to any probability distribution. From the one-sided Chebyshev's inequality [42], as shown in Fig. 8, if RD is a random variable with expectation μ_s or μ_{ns} and variance σ_s^2 or σ_{ns}^2, then for any positive k_{ns} or $k_s > 0$, we have the error rates of early termination and early split by

$$P_s(RD \leq \mu_s - k_s\sigma_s) \leq \frac{1}{1+k_s^2} \tag{9}$$

$$P_{ns}(RD \geq \mu_{ns} + k_{ns}\sigma_{ns}) \leq \frac{1}{1+k_{ns}^2} \tag{10}$$

TABLE 3. The probability for $P_s(RD \le \mu_s - k_s\sigma_s)$ or $P_{ns}(RD \ge \mu_{ns} + k_{ns}\sigma_{ns}$ vs. k_s or k_{ns}.

k_s or k_{ns}	1.5	2	2.5	3	3.5	4	4.5	5	5.5	6
$P_s(RD \le \mu_s - k_s\sigma_s)$ or $P_{ns}(RD \ge \mu_{ns} + k_{ns}\sigma_{ns}$ (%)	30.77	20.00	13.79	10.00	7.55	5.88	4.71	3.85	3.20	2.70

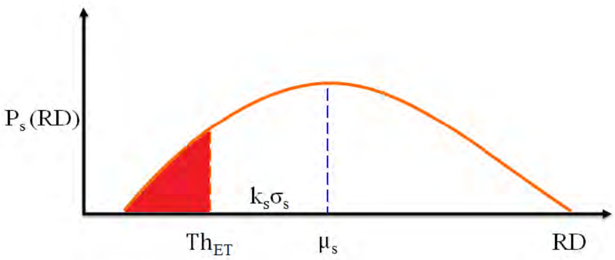

(a) Th_{ET}

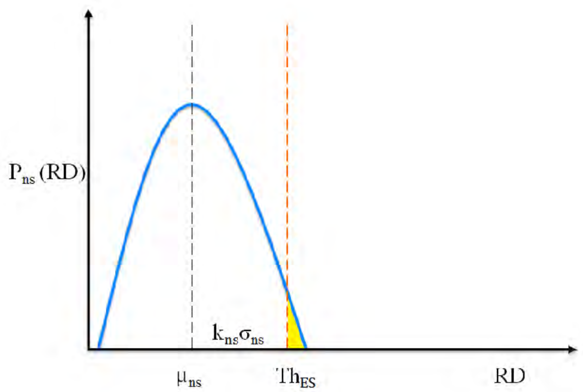

(b) Th_{ES}

FIGURE 8. Illustration of the Th_{ET} and Th_{ES} thresholds by one-sided Chebyshev's inequality. (a) Th_{ET}. (b) Th_{ES}.

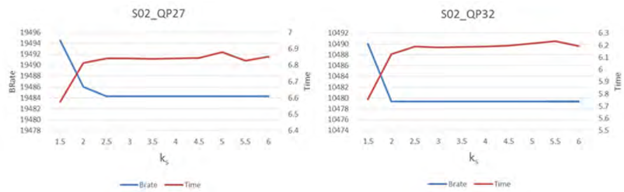

(a)

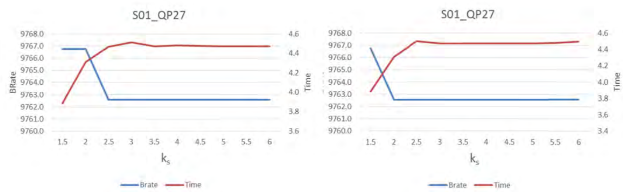

(b)

FIGURE 9. The correlation of coding time and bitrate with various k_s values. (a) Results of Sequence S02 at depth 1 with QP 27 and 32. (b) Results of Sequence S01 at depth 1 and 2 with QP 27.

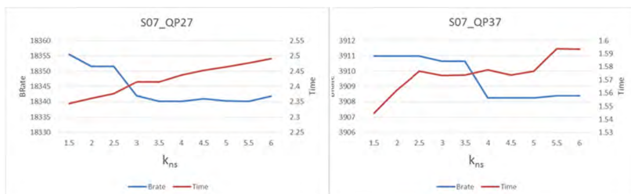

(a)

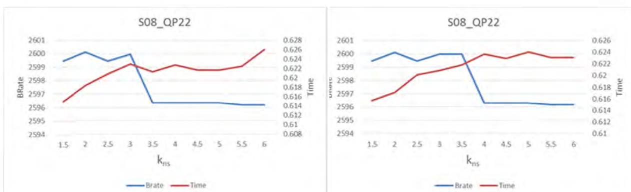

(b)

FIGURE 10. The correlation of coding time and bitrate *with various* k_{ns} *values*. (a) Results of Sequence S07 at depth 1 with QP 27 and 37. (b) Results of Sequence S08 at depth 0 and 1 with QP 22.

In this paper, we apply a one-sided Chebyshev's inequality to obtain the threshold for early termination (Th_{ET}) and the threshold for early split (Th_{ES}) as shown in Fig. 8. They are respectively given by

$$Th_{ET} = \mu_s - k_s\sigma_s \tag{11}$$

$$Th_{ES} = \mu_{ns} + k_{ns}\sigma_{ns} \tag{12}$$

TABLE 3 shows the probability of $P_s(RD \le \mu_s - k_s\sigma_s)$ or $P_{ns}(RD \ge \mu_{ns} + k_{ns}\sigma_{ns})$ with different values of k_s or k_{ns}. When the value of k_s or k_{ns} is larger, the probability of P_s or P_{ns} is lower. In contrast, the probability of $P_s(RD \le \mu_s - k_s\sigma_s)$ or $P_{ns}(RD \ge \mu_{ns} + k_{ns}\sigma_{ns})$ is higher when the value of k_s or k_{ns} is smaller. How to select accurate thresholds for TH_{ET} and TH_{ES} is an essential issue in the proposed algorithm. Applying precise thresholds for the encoder will not only improve the coding speed, but also will maintain the RD performance.

Error rate is the trade-off, and this affects the performance of the encoder. As shown in Fig. 8, the shaded area indicates the error rates of early termination or early split. The larger the value of k_s, the harder it is for early termination by Th_{ET} to be triggered. On the contrary, when the value of k_s is smaller, the error rate is larger and the early termination by Th_{ET} is activated more easily. The threshold Th_{ES} has the same tendency about how it is affected by k_{ns}.

We have analyzed the coding time and bitrate for various values of k_s and k_{ns} to find out accurate values for each CU depth with different QPs as shown in Fig. 9 and Fig. 10, respectively. In Fig. 9 and Fig. 10, the left vertical-axis represents the average bitrate of encoded frames, the right vertical-axis indicates average coding time per frame, and the horizontal-axis shows the values of k_s or k_{ns}.

To select proper k_s and k_{ns}, we set the k_s and k_{ns} values from 1.5 to 6 with an interval of 0.5. We have analyzed the correlation between coding time and bitrate and tried to

TABLE 4. The k_s for various CU depths and various QPs.

QP	Depth=0	Depth=1	Depth=2
22	2.501	1.849	1.689
27	2.286	1.791	1.571
32	2.072	1.732	1.453
37	1.857	1.674	1.335

TABLE 5. The k_{ns} for various CU depths and various QPs.

QP	Depth=0	Depth=1	Depth=2
22	2.380	3.193	3.620
27	2.862	3.679	4.107
32	3.344	4.165	4.595
37	3.825	4.650	5.082

choose suitable k_s and k_{ns} values for the training sequences. The training sequences include S01-S08 with QPs of 22, 27, 37 and 37.

From Fig. 9 and Fig. 10, we try to find out the saturation points of k_s and k_{ns} for various CU depths and various QPs. The saturation point is picked when k_s and k_{ns} increase and the bitrate is no longer declining and coding time is no longer increasing. In the right-hand part of Fig. 9(a), since the bitrate of the k_s with a value of 2.5 shows a tiny advantage in terms of increased coding time over that of the k_s with a value of 2 for QP 32, we select k_s with a value of 2 as a saturation point. The saturation points of k_s value are chosen as 2.5 and 2 for sequence S02 at depth 1 with QP 27 and 32, respectively. For the right-hand part of Fig. 9(b), since the bitrate of the k_s with a value of 2.5 indicates an insignificant gain in terms of increased coding time over that of the k_s with a value of 2, the k_s with a value of 2 is treated as a saturation point. The saturation points of k_s values are chosen as 2.5 and 2 for sequence S01 at depth 1 and 2 with QP 27, respectively.

From the left-hand part of Fig. 10(a), since the bitrate of the k_{ns} with a value of 3.5 indicates a minor advantage in terms of increased coding time over that of the k_{ns} with a value of 3 for QP 27, we select k_{ns} with a value of 3 as a saturation point. The saturation points of k_{ns} are chosen to 3 and 4 for sequence S07 at depth 1 with QP 27 and 37, respectively. For Fig. 10(b), the saturation points of k_{ns} are chosen as 3.5 and 4 for sequence S08 at depth 0 and 1 with QP 22, respectively.

$$\begin{aligned} k_s(S_{CU}, QP) = {} & 2.767 - 0.04121 S_{CU} - 0.03467 QP \\ & + 0.000376 S_{CU}^2 + 0.0006527 S_{CU} QP \\ & - 0.0004333 QP^2 \end{aligned} \tag{13}$$

$$\begin{aligned} k_{ns}(S_{CU}, QP) = {} & 1.9053 - 0.02734 S_{CU} - 0.0979 QP \\ & + 0.00002555 S_{CU}^2 - 0.00002411 S_{CU} QP \\ & - 0.00002564 QP^2 \end{aligned} \tag{14}$$

The final k_s and k_{ns} values have been summarized for 8 sequences according to the CU depths and the different QPs, which are listed in TABLE 4 and TABLE 5, respectively. In TABLE 4, when the QP is getting smaller, the value of k_s is getting larger and the error rate is getting smaller and it is harder for the early termination to be triggered. We intend to ensure that the value of Th_{ET} becomes stricter when the encoding CU has a smaller quantization parameter because a video sequence encoded with a smaller quantization parameter maintains better RD performance compared to that delivered with a larger quantization parameter. Accordingly, the threshold of early termination is not allowed to be loose. This reflects the fact that the encoding CU with a smaller quantization parameter makes early termination by smaller Th_{ET} more difficult, which means that Th_{ET} is set strictly to keep RD efficiency. In addition, when the CU depth is smaller, k_s is also larger. In our opinion, Th_{ET} needs to be set strictly to early terminate the encoding process with large size CUs, so as to avoid RD degradation. Therefore, when encoding large CU or encoding with a small quantization parameter, the value of k_s can be set to be larger and Th_{ET} is set to be strict for early termination in to maintain RD performance.

According to the statistical results from TABLE 5, the value of k_{ns} is smaller when the encoding CU depth or the quantization parameter is smaller. In general, when the RD-cost is relatively large, the value of k_{ns} is set to be smaller for easy early split of the CU coding process when the depth of the current CU is smaller, to speed up the CU coding process.

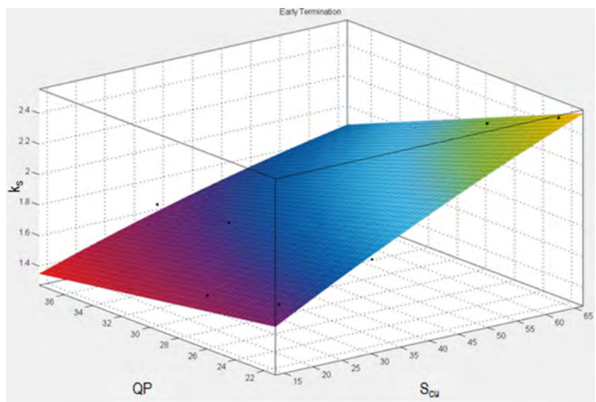

FIGURE 11. The 2-D hyperplane depicting the distribution of Th_{ET}.

To predict Th_{ET}, the sizes of the CU, the QP values and the value of RD-cost are used to build a model according to TABLE 4. A 2-D hyperplane is used to describe the correlation between QP, the size of CU (S_{CU}), and k_s as indicated in Fig. 11. This 2D hyperplane can be represented by an equation in (13). The value of k_s is derived from (13), as shown in TABLE 6. Accordingly, the Th_{ES} follows the same rule to build 2D hyperplane according to TABLE 5 shown in Fig. 12. The hyperplane can be represented by an equation in (14). The value of k_{ns} is derived from (14) as shown in TABLE 7.

In a summary, in this sub-section, we apply a one-sided Chebyshev's inequality to obtain the threshold for early termination ($\boldsymbol{Th_{ET}}$) and the threshold for early split ($\boldsymbol{Th_{ES}}$) as shown in (11) and (12). According to the statistical data, the 2-D hyperplanes are fitted by considering QP variations and CU sizes for acquiring proper parameters ($\boldsymbol{k_s}$ and $\boldsymbol{k_{ns}}$) of $\boldsymbol{Th_{ES}}$

TABLE 6. The distribution of k_s for Th_{ET}.

QP	Depth=0	Depth=1	Depth=2
22	2.5007	1.8487	1.6894
23	2.4578	1.8371	1.6657
24	2.4149	1.8255	1.6421
25	2.3720	1.8138	1.6185
26	2.3291	1.8022	1.5948
27	2.2862	1.7905	1.5712
28	2.2433	1.7789	1.5475
29	2.2004	1.7673	1.5239
30	2.1575	1.7556	1.5002
31	2.1146	1.7440	1.4766
32	2.0717	1.7323	1.4529
33	2.0288	1.7207	1.4293
34	1.9859	1.7091	1.4057
35	1.9431	1.6974	1.3820
36	1.9002	1.6858	1.3584
37	1.8573	1.6741	1.3347
38	1.8144	1.6625	1.3111
39	1.7715	1.6509	1.2874
40	1.7286	1.6392	1.2638
41	1.6857	1.6276	1.2401

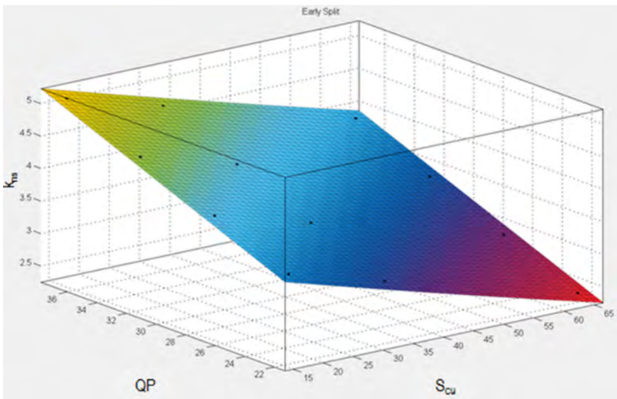

FIGURE 12. The 2-D hyperplane depicting the distribution of Th_{ES}.

TABLE 7. The distribution of k_{ns} for Th_{ES}.

QP	Depth=0	Depth=1	Depth=2
22	2.3800	3.1934	3.6197
23	2.4764	3.2905	3.7172
24	2.5728	3.3877	3.8147
25	2.6691	3.4848	3.9123
26	2.7655	3.5819	4.0098
27	2.8618	3.6791	4.1073
28	2.9582	3.7762	4.2048
29	3.0545	3.8733	4.3023
30	3.1509	3.9704	4.3998
31	3.2473	4.0676	4.4973
32	3.3436	4.1647	4.5949
33	3.4400	4.2618	4.6924
34	3.5363	4.3590	4.7899
35	3.6327	4.4561	4.8874
36	3.7290	4.5532	4.9849
37	3.8254	4.6503	5.0824
38	3.9218	4.7475	5.1799
39	4.0181	4.8446	5.2775
40	4.1145	4.9417	5.3750
41	4.2108	5.0389	5.4725

and Th_{ET}, respectively. The practical employments of Th_{bi}, Th_{ET}, and Th_{ES} in the proposed approach will be introduced in the following sub-sections.

D. ANALYSIS OF PU SIZES

We also intend to explore the correlation between CU depth and PU size in an attempt to reduce the number of prediction modes. We have analyzed the distribution of CU depth and PU size, as shown in TABLE 8 and TABLE 9. In TABLE 8, the SKIP, Merge and Inter 2N × 2N modes occupy 42.0%, 18.0%, and 9.8% of overall PU types for QP 22, respectively. Moreover, according to TABLE 9, the SKIP, Merge, and Inter 2N × 2N modes occupy 61.1%, 8.2%, and 8.9% of overall PU types for QP 37, respectively.

TABLE 8. Distribution of the depth versus PU size for QP 22.

QP=22	Depth=0	Depth=1	Depth=2	Depth=3	Average
Inter SKIP	72.3%	40.6%	31.8%	23.2%	42.0%
Inter Merge	8.0%	18.5%	20.0%	25.6%	18.0%
Inter 2N×2N	6.7%	9.2%	10.5%	13.0%	9.8%
Inter 2N×N	4.2%	6.4%	6.7%	12.3%	7.4%
Inter N×2N	5.0%	7.3%	7.8%	13.9%	8.5%
Inter 2N×nU	0.7%	3.8%	4.6%	0.0%	2.3%
Inter 2N×nD	0.6%	3.3%	3.9%	0.0%	2.0%
Inter nL×2N	1.0%	4.2%	5.2%	0.0%	2.6%
Inter nR×2N	0.8%	3.6%	4.3%	0.0%	2.2%
Intra 2N×2N	0.6%	3.1%	5.3%	8.0%	4.3%
Intra N×N	0.0%	0.0%	0.0%	4.1%	1.0%
Total	100%	100%	100%	100%	100%

TABLE 9. The distribution of the depth versus PU size for QP 37.

QP=37	Depth=0	Depth=1	Depth=2	Depth=3	Average
Inter SKIP	79.8%	59.8%	55.2%	49.6%	61.1%
Inter_Merge	2.9%	7.7%	9.2%	13.0%	8.2%
Inter_2N×2N	8.3%	9.3%	8.8%	9.3%	8.9%
Inter 2N×N	2.7%	3.9%	3.7%	5.1%	3.8%
Inter N×2N	4.0%	5.8%	5.3%	6.5%	5.4%
Inter 2N×nU	0.4%	2.1%	2.0%	0.0%	1.1%
Inter 2N×nD	0.3%	2.0%	1.9%	0.0%	1.1%
Inter nL×2N	0.7%	3.2%	2.8%	0.0%	1.7%
Inter nR×2N	0.6%	2.7%	2.4%	0.0%	1.4%
Intra 2N×2N	0.4%	3.6%	8.6%	12.7%	6.3%
Intra N×N	0.0%	0.0%	0.0%	3.9%	1.0%
Total	100%	100%	100%	100%	100%

TABLE 10 tabulates the average distribution of the depth versus PU size for non-split and split CUs for QP 22, 27, 32, 37. The statistical results confirm that the SKIP, Merge, and Inter 2N × 2N prediction modes have higher probabilities among the prediction modes, whereas the other modes are less likely to occur. In addition, several works [26], [27], [29], [30] propose fast algorithms according to this observation conclusion. Moreover, the non-split CUs tend to select the prediction modes of Skip and Merge as the best mode. In the contrast, the split CUs are more likely to select complex-partitioned prediction modes as the best mode. However, in our opinion, as shown in TABLE 8, the Inter 2N × N and Inter N × 2N prediction modes account for more than 15.9%, on average, of the overall PU types for QP 22, which would seem not to be ignorable. Therefore, we utilize the observed probabilities in this case when the RD-cost of the current encoding CU is less than Th_{bi} and greater than or equal to TH_{ET}.

TABLE 10. Average distribution of the depth versus PU size for non-split and split CU for QP 22, 27, 32, 37.

PU Mode	Non-Split			Split		
	Depth=0	Depth=1	Depth=2	Depth=0	Depth=1	Depth=2
Inter_Skip	73.5%	82.8%	88.2%	27.3%	25.7%	36.5%
Inter_Merge	3.4%	3.8%	3.7%	4.4%	7.3%	8.2%
Inter 2N×2N	6.0%	3.5%	2.5%	6.3%	4.9%	6.0%
Inter 2N×N	5.6%	2.0%	0.7%	13.1%	9.1%	4.7%
Inter N×2N	6.1%	2.0%	0.6%	13.2%	9.3%	4.6%
Inter N×N	0.0%	0.0%	0.0%	0.0%	0.0%	0.0%
Inter 2N×nU	1.0%	1.0%	0.3%	2.2%	4.1%	2.1%
Inter 2N×nD	0.8%	0.8%	0.3%	1.8%	3.5%	1.8%
Inter nL×2N	1.2%	0.9%	0.3%	2.4%	4.2%	2.1%
Inter nR×2N	1.0%	0.8%	0.3%	2.3%	3.7%	1.9%
Intra 2N×2N	1.5%	2.5%	3.2%	27.1%	28.2%	32.1%

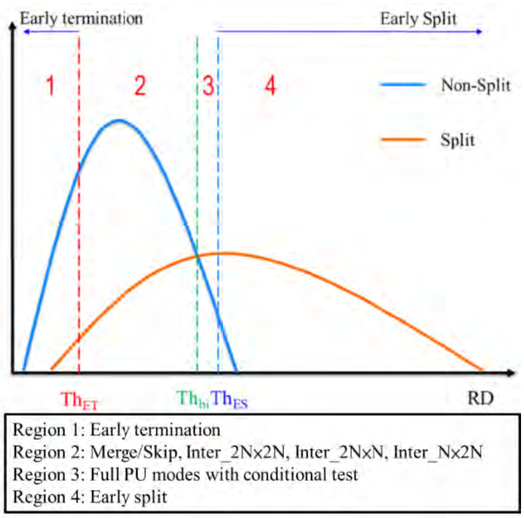

FIGURE 13. The fast PU process for various RD-cost ranges.

The illustration is also shown in Fig. 13. In summary, after Merge/Skip and Inter 2N $\times$ 2N, if the RD-cost of the current CU is less than Th_{ET}, the current CU is early terminated and it proceeds to encode the next CTU; if the RD-cost of the current CU is less than Th_{bi} and greater than or equal to Th_{ET}, the CU coding process further predicts the PU sizes of Inter 2N $\times$ N and Inter N $\times$ 2N; if the RD-cost of the current CU is greater than or equal to Th_{bi} and smaller than Th_{ES}, we predict all of the following PU sizes after conditional test; if the RD-cost of the current CU is greater than or equal to Th_{ES}, the current CU is early split and it proceeds to encode the next CU depth.

E. ANALYSIS OF SEARCH RANGE

In the procedure for encoding a CU, ME occupies most computational power. In HM, the default size of search range is 64.; however, 64 is too large for most cases causing unnecessary computation.

Fig. 14 shows the relevance of search range (SR), coding time and RD performance when SKIP mode is enabled for some test sequences. We conclude that the SR can be reduced with the slight degradation of RD performance.

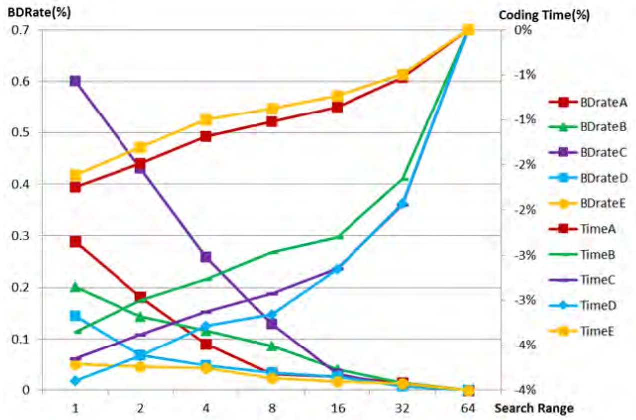

FIGURE 14. Illustration of relevance of search range, coding time and RD performance when SKIP mode is enabled.

To determine the search range precisely, we set the SR to 1, 2 and 4 after Merge/SKIP prediction and the SKIP mode is the current best mode depending on the statistical results in Fig. 14. To verify the assumption, the probabilities that the SR is smaller than or equal to SR in the current depth when the SKIP flag is set after Merge/SKIP prediction are listed in TABLE 11.

TABLE 11. The probability that the search range is smaller than or equal to SR with the enabled skip flag in several training sequences.

Training sequence	Probability (%)		
	SR=1	SR=2	SR=4
Class A	92.60	98.14	98.28
Class B	90.37	96.58	96.61
Class C	93.41	98.24	98.47
Class D	91.97	98.57	98.59
Class E	96.89	98.89	98.90

In TABLE 11, the probability of SR 2 is more than 96 percent. According to Fig. 14, since the probability of SR 4 shows a minor advantage in BDBR with significant time saving compared to that of SR 2, we can speed up the ME for the rest of the prediction modes accordingly to downsize the SR to 2 when the best prediction mode is SKIP mode for unidirectional motion compensation with an estimable RD performance. The SR 4 of bidirectional motion compensation is maintained. Therefore, we apply the probabilities observed in TABLE 11 and conclude that for the case like this, the prediction mode of the current CU is SKIP.

F. OVERALL ALGORITHM

Before introducing the overall algorithm as shown in Fig. 15, several variables are defined as follows.

$Depth_{CU}$: The CU depth of the current CU

$Depth_{pre}$: The predicted CU depth of the current CU by (3)

$Depth_{LBound}$: The executed smallest depth of the current CU

$Depth_{UBound}$: The executed largest depth of the current CU

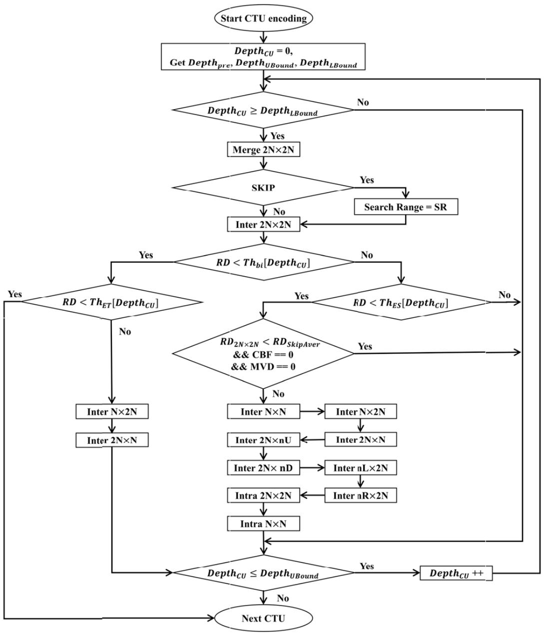

FIGURE 15. Flowchart of the proposed algorithm.

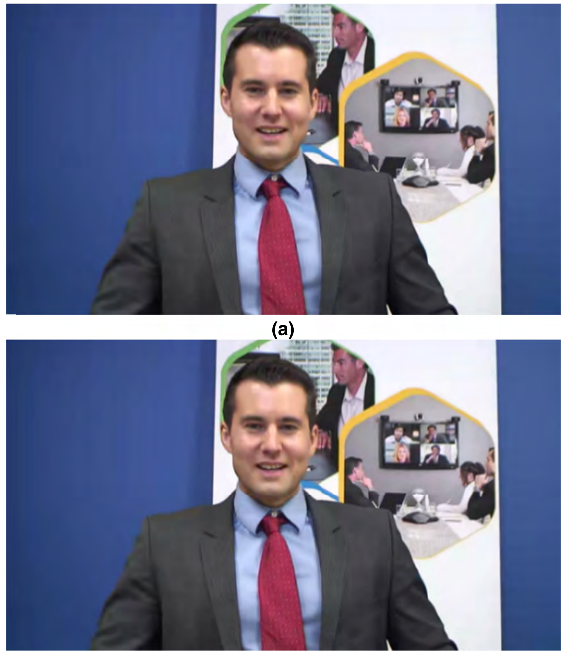

FIGURE 16. Subjective comparison of the 9th frame of Johnny (1280 × 720) sequence for random access configuration (QP 37). (a) HM 12.0, Y-PSNR 37.3458 dB. (b) Proposed, Y-PSNR 37.3224 dB, TS = 72.37%.

$Th_{ET}[Depth_{CU}]$: Threshold of early termination for $\mathrm{Depth_{CU}}$

$Th_{ES}[Depth_{CU}]$: Threshold of early split for $\mathrm{Depth_{CU}}$

$Th_{bi}[Depth_{CU}]$: Binarization threshold for $\mathrm{Depth_{CU}}$

RD: The RD cost of the current best mode

$RD_{2N\times 2N}$: The RD cost of 2N × 2N mode

$RD_{SkipAver}$: The average RD cost of the last 5 SKIP modes in previous CUs

The detailed procedures of the overall algorithm are described step by step as follows.

Step 1: Set $Depth_{CU} = 0$, get $Depth_{pre}$ as the predicted CU depth of the current CU, and $Depth_{LBound}$, $Depth_{UBound}$ as the extended CU depth boundary.

Step 2: If $Depth_{CU} \geq Depth_{LBound}$, go to Step 3. Otherwise, jump to Step 13.

Step 3: Perform Merge/SKIP prediction mode.

Step 4: If the best prediction mode is SKIP mode, jump to Step 5. Otherwise, go to Step 6.

Step 5: Set SR to search range.

Step 6: Perform Inter 2N × 2N prediction mode.

Step 7: If $RD < Th_{bi}[Depth_{CU}]$, go to Step 8, Otherwise, jump to Step 10.

Step 8: If $RD < Th_{ET}[Depth_{CU}]$, jump Step 15, Otherwise, go to Step 9.

Step 9: Check Inter N × 2N, Inter 2N × N and jump to Step 13.

Step 10: If $RD < Th_{ES}[Depth_{CU}]$, go to Step 11. Otherwise, jump to Step 13.

Step 11: If $RD_{2N\times 2N} < RD_{SkipAver}$ && CBF==0 && MVD==0, jump to Step 13. Otherwise go to Step 12.

Step 12: Predict Inter N × N, Inter N × 2N, Inter 2N × N, Inter 2N × nU, Inter 2N × nD, Inter nL × 2N, Inter nR × 2N, Intra 2N × 2N, and Intra N × N and go to Step 13.

Step 13: If $Depth_{CU} \leq Depth_{UBound}$, go to Step 14. Otherwise, jump to Step 15.

Step 14: Add 1 to $Depth_{CU}$, and then jump to Step 2.

Step 15: Move to next CTU.

TABLE 12. configurations of simulation environment.

Configurations	Random Access	Low delay
IntraPeriod	32	-1
GOPSize	8	4
FastSearch	TZSearch	TZSearch
SearchRange	64	64
InternalBitDepth	8	8

IV. SIMULATION RESULTS

TABLE 12 shows the simulation environment [43]. A total of 18 testing sequences from TABLE 1 have been tested with quantization parameters of 22, 27, 37 and 37. The parameters of $\mu_s[Depth_{CU}]$, $\mu_{ns}[Depth_{CU}]$, $\sigma_s[Depth_{CU}]$ and $\sigma_{ns}[Depth_{CU}]$ for $Th_{ET}[Depth_{CU}]$ and $Th_{ES}[Depth_{CU}]$ are updated in each GOP period. The first inter-prediction frame is not applied to fast coding algorithm to get the parameters. The thresholds for $Th_{bi}[Depth_{CU}]$ are pre-trained.

We compare the proposed algorithm with methods in [33]–[38]. TABLE 13 and TABLE 14 show the coding performance comparisons for the random access and low delay configuration, respectively. For the random access configuration in TABLE 13, the proposed algorithm has the same

TABLE 13. Coding performance comparisons of the proposed algorithm and [33]–[38] for random access configuration.

			[33] HM-12.0		[34] HM-12.0		[35] HM-16.5		[36] HM-12.0		[37] HM-10.0		[38] HM-13.0		Proposed, HM-12.0	
Class	Sequence		BD BR (%)	TS (%)	BD BR (%)	TS (%)	BD BR (%)	TS (%)	BD BR (%)	TS (%)	BD BR (%)	TS (%)	BD BR (%)	TS (%)	BD BR (%)	TS (%)
Class A 2560x1600	S01	Traffic	1.1	60.5	0.8	61.6	2.0	60.3	0.6	31.4	0.2	43.6			1.2	55.1
	S02	PeopleOnStreet	0.2	42.5	0.9	26.9	2.8	47.2	1.2	32.5	0.7	42.3			1.7	51.9
		Average	0.7	51.5	0.9	44.3	2.4	53.8	0.9	32.0	0.5	43.0			1.5	53.5
Class B 1920×1080	S03	Kimono	1.0	47.3	1.3	58.2	2.4	57.1			0.3	46.3	0.8	52.0	1.2	52.2
	S04	ParkScene	0.9	45.2	1.2	52.6	2.3	58.3	0.6	30.6			0.5	49.6	1.3	51.7
	S05	Cactus	1.0	42.1	2.8	56.8	3.0	56.7	0.6	31.6	0.5	42.4	1.1	48.6	1.2	50.6
	S06	BasketballDrive	1.0	41.8	2.0	50.9	3.8	57.0	0.8	31.1	0.4	43.1	1.1	51.4	1.8	54.1
	S07	BQTerrace	1.1	49.7	1.6	54.5	1.5	59.8	0.6	28.0	0.5	47.9	0.4	44.8	1.0	51.8
		Average	1.0	45.2	1.8	54.6	2.6	57.8	0.6	30.3	0.4	44.9	0.8	49.3	1.3	52.1
Class C 832×480	S08	BasketballDrill	2.1	39.8	1.9	45.2	3.1	57.6	0.7	30.6	0.5	36.0	0.7	48.6	1.0	38.2
	S09	BQMall	1.6	40.0	2.2	48.6	3.8	55.8	1.1	29.5	0.5	40.3	1.6	45.9	1.4	48.3
	S10	PartyScene	1.1	45.8	0.8	37.7	1.9	54.0	1.0	25.6	0.3	38.0	0.9	46.3	0.9	43.1
	S11	RaceHorses	1.8	38.5	2.2	33.9	3.0	51.4	1.8	30.4			2.2	46.6	1.2	37.4
		Average	1.7	41.0	1.8	41.4	3.0	54.7	1.1	29.0	0.4	38.1	1.4	46.8	1.1	41.8
Class D 416×240	S12	BasketballPass	1.8	28.9	1.5	33.6	3.3	55.8	1.0	30.0	0.4	32.5	2.1	49.3	0.8	39.2
	S13	BQSquare	0.4	34.4	0.6	45.4	1.3	58.3	0.9	24.4	0.5	56.3	1.6	44.5	0.6	43.0
	S14	BlowingBubbles	1.3	33.7	0.7	38.2	2.5	52.4	1.0	27.1	0.3	40.3	1.4	42.0	0.9	43.4
	S15	RaceHorses	1.8	24.4	1.1	26.6	3.3	48.3			0.7	29.0	2.0	42.2	1.7	48.2
		Average	1.3	30.4	1.0	36.0	2.6	53.7	1.0	27.2	0.5	39.5	1.8	44.5	1.0	43.5
Class E 1280×720		FourPeople	1.4	66.3	1.7	74.1									1.0	62.3
		Johnny	0.9	67.8	1.3	75.7									1.0	69.2
		KristenAndSara	1.3	62.5	1.2	73.1									1.1	62.3
		Average	1.2	65.5	1.4	74.3									1.0	64.6
Total Average			1.2	45.1	1.4	49.6	2.7	55.3	0.9	29.4	0.4	41.4	1.3	47.1	1.2	50.1

TABLE 14. Coding performance Comparisons of the proposed algorithm and Three individual methods for random access configuration.

			[33] HM-12.0		[34] HM-12.0		[35] HM-16.5		[36] HM-12.0		[37] HM-10.0		[38] HM-13.0		Proposed, HM-12.0	
Class	Sequence		BD BR (%)	TS (%)	BD BR (%)	TS (%)	BD BR (%)	TS (%)	BD BR (%)	TS (%)	BD BR (%)	TS (%)	BD BR (%)	TS (%)	BD BR (%)	TS (%)
Class A 2560x1600	S01	Traffic	1.0	54.7	2.0	41.7									1.1	52.5
	S02	PeopleOnStreet	0.4	32.5	1.5	28.0									1.1	52.0
		Average	0.7	43.6	1.8	34.9									1.1	52.3
Class B 1920×1080	S03	Kimono	0.8	38.0	0.8	47.9	2.6	60.5			0.3	46.5	0.9	54.2	0.8	50.0
	S04	ParkScene	0.8	40.5	1.1	48.3	2.7	56.5	1.0	36.7			0.6	51.3	1.3	49.5
	S05	Cactus	0.5	43.5	2.2	48.0	3.2	59.3	0.7	36.9	0.4	42.8	1.2	48.5	1.1	50.4
	S06	BasketballDrive	0.8	42.3	1.2	42.6	3.5	59.4	1.0	39.4	0.4	40.2	0.5	54.0	1.4	52.4
	S07	BQTerrace	1.3	42.7	0.3	47.5	2.2	58.7	1.1	33.8	0.3	46.8	0.5	45.1	1.3	51.4
		Average	0.8	41.4	1.1	46.9	2.8	58.9	1.0	36.7	0.4	44.1	0.7	50.6	1.2	50.7
Class C 832×480	S08	BasketballDrill	1.9	44.0	2.0	37.0	3.3	58.9	0.9	37.9	0.4	30.5	1.0	49.8	1.0	37.5
	S09	BQMall	2.0	43.5	1.2	40.9	3.7	55.7	1.2	37.7	0.6	35.0	2.0	45.9	1.1	47.9
	S10	PartyScene	1.0	40.0	0.4	33.0	2.2	52.5	1.4	34.3	0.6	36.4	1.5	45.5	1.0	41.2
	S11	RaceHorses	1.0	34.1	1.1	26.1	2.5	51.1	1.5	40.9			2.2	52.0	1.1	40.9
		Average	1.5	40.4	1.2	34.3	2.9	54.6	1.2	37.7	0.5	33.9	1.7	48.3	1.1	41.9
Class D 416×240	S12	BasketballPass	1.5	35.4	1.2	27.7	2.9	55.9	1.1	39.2	0.6	27.6	2.3	53.6	0.9	42.6
	S13	BQSquare	0.4	36.0	0.2	38.8	1.7	53.3	2.3	31.8	0.7	35.7	2.1	45.5	1.0	40.3
	S14	BlowingBubbles	2.2	39.8	0.3	31.5	2.5	51.4	1.7	36.2	0.4	31.8	2.1	49.7	0.9	38.7
	S15	RaceHorses	0.7	30.8	0.7	21.2	2.7	47.9			0.6	24.9	2.5	48.3	1.3	48.3
		Average	1.2	35.5	0.6	29.8	2.5	52.1	1.7	35.7	0.6	30.0	2.3	49.3	1.0	42.5
Class E 1280×720		FourPeople	1.1	64.0	1.6	65.6	2.8	70.3	0.5	37.6	0.6	50.6			0.9	58.6
		Johnny	1.3	66.9	-0.3	73.9	3.9	69.8	1.2	37.6	0.7	53.0			0.9	64.3
		KristenAndSara	1.4	60.9	0.5	69.6	3.0	69.6	0.9	38.3	0.4	51.8			0.6	57.6
		Average	1.3	64.9	0.6	69.7	3.2	69.9	0.9	37.8	0.6	51.8			0.8	60.2
Total Average			1.1	43.9	1.0	42.7	2.8	58.2	1.2	37.0	0.5	39.5	1.5	49.5	1.0	48.7

average BDBR performance by 1.2% with better average time saving by 50.1% compared to 45.1% in [33]. Moreover, the proposed algorithm provides less BDBR degradation and better time saving (1.2% and 50.1%) at the same time compared to that of (1.4% and 49.6%) in [34] and (1.3% and 47.1%) in [38]. The BDBR increases in [36] and [37], 0.9% and 0.4%, are just slightly lower than our approach; however, we make a significant progress on time saving by

TABLE 15. Coding performance comparisons of the proposed algorithm and [33]–[38] for low delay configuration.

HM 12.0		CU Depth Estimation			Early Termination and Early Split			Search Range Adjustment		
Class	Sequence	BD BR (%)	BD PSNR (dB)	TS (%)	BD BR (%)	BD PSNR (dB)	TS (%)	BD BR (%)	BD PSNR (dB)	TS (%)
A	S01	0.09	-0.005	17.58	1.16	-0.039	43.43	0.00	0.00	5.01
	S02	0.10	-0.005	17.60	1.64	-0.073	38.29	0.05	-0.002	4.68
	Average	0.10	-0.005	17.59	1.40	-0.056	40.86	0.03	-0.001	4.85
B	S03	0.11	-0.004	16.40	1.16	-0.035	39.34	0.06	-0.002	5.80
	S04	0.11	-0.005	16.95	1.24	-0.039	41.41	0.02	-0.001	5.59
	S05	0.12	-0.004	17.53	1.08	-0.013	39.29	0.06	-0.002	3.95
	S06	0.06	-0.002	17.96	1.75	-0.038	42.61	0.07	-0.002	5.96
	S07	0.13	-0.008	18.16	0.91	-0.014	37.57	0.10	-0.002	4.89
	Average	0.11	-0.005	17.40	1.23	-0.028	40.04	0.06	-0.002	5.24
C	S08	0.12	-0.006	31.16	0.96	-0.040	30.79	0.05	-0.002	4.01
	S09	0.15	-0.009	16.90	1.41	-0.054	39.64	0.03	-0.001	6.05
	S10	0.27	-0.021	17.10	0.79	-0.034	32.58	0.03	-0.001	2.82
	S11	0.08	-0.005	17.02	1.03	-0.038	26.07	0.07	-0.003	5.80
	Average	0.16	-0.010	20.55	1.05	-0.042	32.27	0.05	-0.002	4.67
D	S12	0.09	-0.005	14.22	0.81	-0.039	31.68	0.09	-0.004	3.95
	S13	0.30	-0.026	14.91	0.53	-0.020	32.58	0.05	-0.002	4.24
	S14	0.16	-0.010	14.65	0.86	-0.036	32.42	0.03	-0.001	2.51
	S15	0.20	-0.013	14.32	1.55	-0.072	33.58	0.10	-0.005	4.37
	Average	0.19	-0.014	14.53	0.94	-0.042	32.57	0.07	-0.003	3.77
E	FourPeople	0.11	-0.006	22.48	0.99	-0.037	45.79	0.01	0.00	1.10
	Johnny	0.14	-0.006	21.16	0.92	-0.022	48.50	0.01	0.00	1.64
	KristenAndSara	0.18	-0.009	21.84	1.17	-0.037	41.60	0.06	-0.002	1.70
	Average	0.14	-0.007	21.83	1.03	-0.032	45.30	0.03	-0.001	1.48
Total Average		0.14	-0.008	18.22	1.11	-0.038	37.62	0.05	-0.002	4.12

50.1% compared to the limited results of 29.4% in [36] and 41.4 in [37]. In addition, the average time saving in [35] is upgraded at the cost of dramatically BDBR degradation by 2.7%, which is not solid enough to guarantee video quality when accelerating the coding process.

The proposed algorithm has stable time saving and coding performance, no matter high or low motion, or high or low resolution. For the S11 RaceHorses sequence with fast moving objects, the BDBR is still 1.2%, which is much better than 1.8% in [33], 3.0% in [35], and 2.2% in [38]. Moreover, the BDBRs are dramatically boosting and the time savings are condensed in [34] (BDBR: 2.2%, TS: 33.9%) and in [36] (BDBR: 1.8%, TS: 30.4%). For the S12 BasketballPass sequence, the time saving of the proposed algorithm is 39.2% with a 0.8% BDBR increase, which is better than the 28.9% time saving with a 1.8% BDBR increase in [33], the 33.6% time saving with a 1.5% BDBR increase in [34], and the 30.0% time saving with a 1.0% BDBR increase in [36]. For low resolution test sequences, such as Class C and D, the time saving and the BDBR of the proposed algorithm are better than those of [33]–[35]. Reference [38] improves the time-saving at the cost of poor BDBR performances. On average, the proposed algorithm maintains a BDBR increase of 1.2% with 50.1% time-saving for random access configuration.

According to TABLE 14, the proposed algorithm for low delay configuration yields 48.7% time saving with a 1.0% BDBR increase, which is better than 43.9% time-saving with a 1.1% BDBR increase of [33]. The time saving of the proposed algorithm is 48.7% compared to 42.7% time saving of [34] under a similar BDBR. For sequences of Class A with high resolution and Class C with low resolution, the BDBR and the time saving of the proposed algorithm are better than those of [34]. For the S03 Kimono sequence, the proposed algorithm can achieve a time saving of about 50.0% compared to the 38.0% of [33] and 47.9% of [34] with similar BDBR performance. For the S08 BasketballDrill sequence with low resolution and high motion, the BDBR is about 1.0% compared to the 1.9% of [33] and the 2.0% of [34]. For the S11 RaceHorses sequence, the time saving is about 40.9%, which is much better than the 34.1% of [33] and 26.1% of [34], with similar RD performance. The average time-saving contribution of [36] and [37] (37.0% and 39.5%) are limited compared to our approach. In addition, the BDBRs of [35] and [38] explode under expectation generally. The average time savings for all classes with low delay configuration have a similar tendency with those of random access configuration. The proposed algorithm can maintain stable time saving and BDBR for various test sequences.

Fig. 16 visually depicts the subjective comparisons for random access configuration. The subjective comparison for low delay configuration is presented in Fig. 17. These figures show that the proposed algorithm can maintain the PSNR quality and increase the time saving significantly.

TABLE 15 shows the coding performance of the proposed algorithm with thee individual methods, namely CU depth estimation, early termination and early split and search range

(a)

(b)

FIGURE 17. Subjective comparison of the 3rd frame of RaceHorses (832 × 480) sequence for low delay configuration (QP 22). (a) HM 12.0, Y-PSNR 39.8937 dB. (b) Proposed, Y-PSNR 39.8856 dB, TS = 42.56%.

adjustment. From this table, we observe that early termination and early split contribute most of performance improvement. The CU depth estimation, which includes step 2 and step 13, offers an 18.22% time saving. The early termination and early split which contain steps 7, 8, 10, 11 provide a 37.62% time saving. Step 5 is used in the third approach and results in a 4.12% time saving.

V. CONCLUSIONS

To relieve the high computational demand of inter-prediction in the encoder of HEVC/H.265, a fast algorithm is proposed. The depth correlation between the current CU and the collocated CU is used to exclude irrelevant CU procedures. We consider the correlation between CU depth and PU size, and accordingly some prediction types can be curtailed. We also explore the distributions of the Rate-Distortion costs (RD-costs) between the final best CUs (Non-split CU) and the CUs to be further split (Split CU), and then we present bimodal RD-cost segmentation incorporated with automatic Otsu thresholding. By evaluating different CU sizes and QPs, we have built mathematical models using a one-sided Chebyshev's inequality method to adjust the thresholds by accurately estimating the error rate for early split and early termination mechanisms. In addition, SR reduction is used to further accelerate the coding process.

Experimental results show our algorithm achieves the best coding time saving up to 69.2%, and the averages of coding time savings are 50.1%, and 48.7%, for random access and low delay configurations, respectively. The proposed algorithm has similar coding performance to that of HM 12.0 and performs better than previous works.

REFERENCES

[1] Y.-W. Chen, K. Chen, S.-Y. Yuan, and S.-Y. Kuo, "Moving object counting using a tripwire in H.265/HEVC bitstreams for video surveillance," *IEEE Access*, vol. 4, pp. 2529–2541, May 2016.

[2] Y. Huo, C. Zhou, J. Jiang, and L. Hanzo, "Historical information aware unequal error protection of scalable HEVC/H.265 streaming over free space optical channels," *IEEE Access*, vol. 4, pp. 5659–5672, Aug. 2016.

[3] R. Perera, H. K. Arachch, M. A. Imran, and P. Xiao, "Extrinsic information modification in the turbo decoder by exploiting source redundancies for HEVC video transmitted over a mobile channel," *IEEE Access*, vol. 4, pp. 7186–7198, Oct. 2016.

[4] G. J. Sullivan, J.-R. Ohm, W.-J. Han, and T. Wiegand, "Overview of the high efficiency video coding (HEVC) standard," *IEEE Trans. Circuits Syst. Video Technol.*, vol. 22, no. 12, pp. 1649–1668, Dec. 2012.

[5] T. Wiegand, G. J. Sullivan, G. Bjøntegaard, and A. Luthra, "Overview of the H.264/AVC video coding standard," *IEEE Trans. Circuits Syst. Video Technol.*, vol. 13, no. 7, pp. 560–576, Jul. 2003.

[6] F. Bossen, B. Bross, K. Sühring, and D. Flynn, "HEVC complexity and implementation analysis," *IEEE Trans. Circuits Syst. Video Technol.*, vol. 22, no. 12, pp. 1685–1696, Dec. 2012.

[7] K. Choi, S. H. Park, and E. S. Jang, *Coding Tree Pruning Based CU Early Termination*, document JCTVC-F092, Torino, Italy, Jul. 2011.

[8] J. Yang, J. Kim, K. Won, H. Lee, and B. Jeon, *Early Skip Detection for HEVC*, document JCTVC-G543, Geneva, Switzerland, Nov. 2011.

[9] R. H. Gweon and Y. L. Lee, *Early Termination of CU Encoding to Reduce HEVC Complexity*, document JCTVC-F045, Torino, Italy, Jul. 2011.

[10] X. Deng, M. Xu, and C. Li, "Hierarchical complexity control of HEVC for live video encoding," *IEEE Access*, vol. 4, pp. 7014–7027, Sep. 2016.

[11] Z. Zhang, T. Jing, J. Han, Y. Xu, and F. Zhang, "A new rate control scheme for video coding based on region of interest," *IEEE Access*, vol. 5, pp. 13677–13688, 2017.

[12] S.-C. Tai, C.-Y. Chang, B.-J. Chen, and J.-F. Hu, "Speeding up the decisions of quad-tree structures and coding modes for HEVC coding units," in *Proc. Int. Comput. Symp.*, Dec. 2012, pp. 393–401.

[13] J. Kim, J. Yang, K. Won, and B. Jeon, "Early determination of mode decision for HEVC," in *Proc. Picture Coding Symp. (PCS)*, May 2012, pp. 449–452.

[14] H.-M. Yoo and J.-W. Suh, "Fast coding unit decision based on skipping of inter and intra prediction units," *Electron. Lett.*, vol. 50, no. 10, pp. 750–752, May 2014.

[15] H. L. Tan, F. Liu, Y. H. Tan, and C. Yeo, "On fast coding tree block and mode decision for high-Efficiency Video Coding (HEVC)," in *Proc. IEEE Int. Conf. Acoust., Speech Signal Process. (ICASSP)*, Mar. 2012, pp. 825–828.

[16] J. Kim, S. Jeong, S. Cho, and J. S. Choi, "Adaptive coding unit early termination algorithm for HEVC," in *Proc. IEEE Int. Conf. Consum. Electron. (ICCE)*, Jan. 2012, pp. 261–262.

[17] L. Shen, Z. Liu, X. Zhang, W. Zhao, and Z. Zhang, "An effective CU size decision method for HEVC encoders," *IEEE Trans. Multimedia*, vol. 15, no. 2, pp. 465–470, Feb. 2013.

[18] J. Xiong, H. Li, Q. Wu, and F. Meng, "A fast HEVC inter CU selection method based on pyramid motion divergence," *IEEE Trans. Multimedia*, vol. 16, no. 2, pp. 559–564, Feb. 2014.

[19] M. B. Cassa, M. Naccari, and F. Pereira, "Fast rate distortion optimization for the emerging HEVC standard," in *Proc. Picture Coding Symp. (PCS)*, May 2012, pp. 493–496.

[20] J. Xiong, H. Li, F. Meng, S. Zhu, Q. Wu, and B. Zeng, "MRF-based fast HEVC inter CU decision with the variance of absolute differences," *IEEE Trans. Multimedia*, vol. 16, no. 8, pp. 2141–2153, Dec. 2014.

[21] J. Lee, S. Kim, K. Lim, and S. Lee, "A fast CU size decision algorithm for HEVC," *IEEE Trans. Circuits Syst. Video Technol.*, vol. 25, no. 3, pp. 411–421, Mar. 2015.

[22] J. Leng, L. Sun, T. Ikenaga, and S. Sakaida, "Content based hierarchical fast coding unit decision algorithm for HEVC," in *Proc. Int. Conf. Multimedia Signal Process. (ICMSP)*, May 2011, pp. 56–59.

[23] J.-H. Lee, C.-S. Park, and B.-G. Kim, "Fast coding algorithm based on adaptive coding depth range selection for HEVC," in *Proc. IEEE Int. Conf. Consum. Electron. (ICCE)*, Berlin, Germany, Sep. 2012, pp. 31–33.

[24] G. Correa, P. Assuncao, L. A. da Silva Cruz, and L. Agostini, "Dynamic tree-depth adjustment for low power HEVC encoders," in *Proc. 19th IEEE Int. Conf. Electron., Circuits Syst. (ICECS)*, Dec. 2012, pp. 564–567.

[25] T. Zhao, Z. Wang, and S. Kwong, "Flexible mode selection and complexity allocation in High Efficiency Video Coding," *IEEE J. Sel. Topics Signal Process.*, vol. 7, no. 6, pp. 1135–1144, Dec. 2013.

[26] J. Vanne, M. Viitanen, and T. D. Hamalainen, "Efficient mode decision schemes for HEVC inter prediction," *IEEE Trans. Circuits Syst. Video Technol.*, vol. 24, no. 9, pp. 1579–1593, Sep. 2014.
[27] J. Xiong, H. Li, F. Meng, Q. Wu, and K. N. Ngan, "Fast HEVC inter CU decision based on latent SAD estimation," *IEEE Trans. Multimedia*, vol. 17, no. 12, pp. 2147–2159, Dec. 2015.
[28] G. Corrêa, P. A. Assuncao, L. V. Agostini, and L. A. da Silva Cruz, "Fast HEVC encoding decisions using data mining," *IEEE Trans. Circuits Syst. Video Technol.*, vol. 25, no. 4, pp. 660–673, Apr. 2015.
[29] J. Zhang, B. Li, and H. Li, "An efficient fast mode decision method for inter prediction in HEVC," *IEEE Trans. Circuits Syst. Video Technol.*, vol. 26, no. 8, pp. 1502–1515, Aug. 2016.
[30] N. Hu and E.-H. Yang, "Fast inter mode decision for HEVC based on transparent composite model," in *Proc. IEEE Int. Conf. Image Process. (ICIP)*, Sep. 2015, pp. 1533–1537.
[31] A. Jiménez-Moreno, E. Martínez-Enríquez, and F. Díaz-de-María, "Complexity control based on a fast coding unit decision method in the HEVC video coding standard," *IEEE Trans. Multimedia*, vol. 18, no. 4, pp. 563–575, Apr. 2016.
[32] Y. Zhang, Z. Pan, N. Li, X. Wang, G. Jiang, and S. Kwong, "Effective data driven coding unit size decision approaches for HEVC INTRA coding," *IEEE Trans. Circuits Syst. Video Technol.*, vol. 28, no. 11, pp. 3208–3222, Nov. 2018.
[33] L. Shen, Z. Zhang, and Z. Liu, "Adaptive inter-mode decision for HEVC jointly utilizing inter-level and spatiotemporal correlations," *IEEE Trans. Circuits Syst. Video Technol.*, vol. 24, no. 10, pp. 1709–1722, Oct. 2014.
[34] S. Ahn, B. Lee, and M. Kim, "A novel fast CU encoding scheme based on spatiotemporal encoding parameters for HEVC inter coding," *IEEE Trans. Circuits Syst. Video Technol.*, vol. 25, no. 3, pp. 422–435, Mar. 2015.
[35] L. Zhu, Y. Zhang, S. Kwong, X. Wang, and T. Zhao, "Fuzzy SVM-based coding unit decision in HEVC," *IEEE Trans. Broadcast.*, vol. 64, no. 3, pp. 681–694, Sep. 2018.
[36] Z. Pan, P. Jin, J. Lei, Y. Zhang, X. Sun, and S. Kwong, "Fast reference frame selection based on content similarity for low complexity HEVC encoder," *J. Vis. Commun. Image Represent.*, vol. 40, pp. 516–524, Oct. 2016.
[37] K. Goswami, J.-H. Lee, and B.-G. Kim, "Fast algorithm for the high efficiency video coding (HEVC) encoder using texture analysis," *Inf. Sci.*, vols. 364–365, pp. 72–90, Oct. 2016.
[38] T.-H. Tsai, S. S. Su, and T.-Y. Lee, "Fast mode decision method based on edge feature for HEVC inter-prediction," *IET Image Process.*, vol. 12, no. 5, pp. 644–651, Apr. 2018.
[39] K. H. Tai, M. J. Chen, and X. Z. Li, "Content adaptive intra prediction algorithm for HEVC encoder," *J. Internet Technol.*, vol. 17, no. 3, pp. 509–618, May 2016.
[40] N. Otsu, "A threshold selection method from gray-level histograms," *IEEE Trans. Syst., Man, Cybern.*, vol. SMC-9, no. 1, pp. 62–66, Jan. 1979.
[41] A. W. Marshall and I. Olkin, "A one-sided inequality of the Chebyshev type," *Ann. Math. Statist.*, vol. 31, no. 2, pp. 488–491, 1960.
[42] P. Mukhopadhyay, *An Introduction to the Theory of Probability*. Singapore: World Scientific, 2012.
[43] *HEVC Reference Software Version HM 12.0.* Accessed: Jan. 20, 2016. [Online]. Available: https://hevc.hhi.fraunhofer.de/svn/svn_HEVC Software/tags/HM-12.0

KUANG-HAN TAI received the M.S. and Ph.D. degrees from the Department of Electrical Engineering, National Dong Hwa University, Hualien, Taiwan, in 2012 and 2016, respectively. He is currently an Engineer with Hwacom Systems Inc., Taipei, Taiwan. His research interests include video/image compression and fast algorithms for high efficiency video coding (HEVC).

MEI-JUAN CHEN (M'97–SM'11) received the B.S., M.S., and Ph.D. degrees in electrical engineering from National Taiwan University, Taipei, in 1991, 1993, and 1997, respectively.

She was an Assistant Professor, from 1997 to 2000, and an Associate Professor, from 2000 to 2005, with the Department of Electrical Engineering, National Dong Hwa University, Hualien, Taiwan. From 2005 to 2006, she was the Chair of the Department of Electrical Engineering, National Dong Hwa University, where she has been a Professor, since 2005. Her research topics include image/video processing, video compression, motion estimation, error concealment, and video transcoding. She was a recipient of the dragon paper awards and the Xeror Paper Award, in 1993 and 1997. She received the 2005 K. T. Li Young Researcher Award from the ACM Taipei/Taiwan Chapter for her contribution to video signal codec technique, and this award is given annually to only one person under the age of 36, conducting research in Taiwan. She received the Distinguished Young Engineer Award from the Chinese Institute of Electrical Engineering, Taiwan, in 2006, the Excellent Ph.D./Master Thesis Supervision awards from the Institute of Information and Computer Machinery, in 2006, 2016, and 2017, the Jun S. Huang Memorial Foundation Best Paper awards, in 2005 and 2012, the IPPR Society Best Paper awards, in 2013, 2015, and 2016, the Best and Excellent Master Thesis Supervision awards from the Taiwan Institute of Electrical and Electronic Engineering, in 2011, 2014, 2015, and 2016, the Best Paper Award from the National Symposium on Telecommunication, in 2014, the Best Paper awards from the Taiwan Academic Network Conference, in 2016 and 2017, the First Place of the Best Paper Award from the 2017 IEEE International Conference on Consumer Electronics–Taiwan. She serves as an Associate Editor for the *EURASIP Journal on Advances in Signal Processing*, the *International Journal of Electronics and Information Engineering*, and the *International Journal of Electrical Engineering*.

JIE-RU LIN received the B.S. and M.S. degrees from the Department of Electrical Engineering, National Dong Hwa University, Hualien, Taiwan, in 2015 and 2016, respectively, where he is currently pursuing the Ph.D. degree. From 2018 to 2019, he was a Lecturer. His research interests include fast algorithm and performance improvement of high efficiency video coding (HEVC) and 3D-HEVC. He received the Best Paper Award from the National Symposium on Telecommunication, in 2014, the Best Paper Award from the IPPR Society, in 2016, the Excellent Master Thesis Award from the Taiwan Institute of Electrical and Electronic Engineering, the best paper awards from the Taiwan Academic Network Conference, in 2016 and 2017, and the First Place of the Best Paper Award from the 2017 IEEE International Conference on Consumer Electronics–Taiwan.

REN-YUAN HUANG received the B.S. degree in electrical engineering from National Ilan University, Yilan, Taiwan, in 2010, and the M.S. degree in electrical engineering from National Dong Hwa University, Hualien, Taiwan, in 2013, where he is currently pursuing the Ph.D. degree in electrical engineering. His current research interests include the microwave/RF active circuit design, including mixer, LNA, voltage-controlled oscillator (VCO), QVCO, and video coding.

CHIA-HUNG YEH (M'03–SM'12) received the B.S. and Ph.D. degrees from the Department of Electrical Engineering, National Chung Cheng University, Chiayi, Taiwan, in 1997 and 2002, respectively. He was an Assistant Professor, from 2007 to 2010, an Associate Professor, from 2010 to 2013, and a Professor, from 2013 to 2017, with the Department of Electrical Engineering, National Sun Yat-sen University, Kaohsiung, Taiwan. He is currently a Distinguished Professor with National Taiwan Normal University, Taipei, Taiwan, and the Vice Dean of the College of Technology and Engineering. He has coauthored more than 250 technical international conferences and journal papers. He holds 47 patents in USA, Taiwan, and China. His research interests include multimedia, video communication, 3-D reconstruction, video coding, image/video processing, and big data. He became a Fellow of IET, in 2017. He was a recipient of the 2013 IEEE MMSP Top 10% Paper Award, the 2014 IEEE GCCE Outstanding Poster Award, the 2015 APSIPA Distinguished Lecture, the 2016 NARLabs Technical Achievement Award: Superior Achievement Award, the 2017 IEEE SPS Tainan Section Chair, and the IEEE Outstanding Technical Achievement Award (IEEE Tainan Section). He received the 2007 Young Researcher Award from NSYSU, the 2011 Distinguished Young Engineer Award from the Chinese Institute of Electrical Engineering, the 2013 Distinguished Young Researcher Award from NSYSU, and the 2017 Distinguished Professor Award from NTNU. He was an Associate Editor of the *Journal of Visual Communication and Image Representation*, the *EURASIP Journal on Advances in Signal Processing*, and the *APSIPA Transactions on Signal and Information Processing*. He has been an Active TC Member of the IEEE Communication Society on Multimedia Communication, APSIPA, and IWAIT. He is also one of the founding members of the ACM SIGMM Taiwan Chapter. He served as a Program Co-Chair for the IEEE Big Data Multimedia 2016, the IWAIT&IFMIA 2015, the ICS 2014, the ICICS 2013, the APSIPA 2013, the ICS2012, and the IEEE ISIC 2012, and as a Co-Chair for the IEEE-TW 2016/2015, the IEEE ICME 2014, the CVGIP2012, the IEEE PCM2012, the VCIP 2012, the APSIPA 2012, the CVGIP2011, and the VCIP 2010. He has been on the Best Paper Award Committee of JVCI and APSIPA.

CHIA-YEN CHEN (M'13) received the B.S., M.S. (Hons.), and Ph.D. degrees from the Department of Computer Science, The University of Auckland, New Zealand, in 1996, 1999, and 2004, respectively. She was a Lecturer with the Department of Computer Science, The University of Auckland, from 2002 to 2006. In 2006, she joined the Department of Electrical Engineering, National Chung Cheng University, Taiwan, as an Assistant Professor. She was with the Department of Computer Science and Information Engineering, National University of Kaohsiung, as an Assistant Professor, from 2007 to 2013, and as an Associate Professor, from 2013 to 2017. She was appointed as an Adjunct Associate Professor with National Sun Yat-sen University, for her research in 3-D modeling and augmented reality, from 2014 to 2016. In 2017, she re-joined the Department of Computer Science, The University of Auckland, as a Lecturer. Since 2007, she has received and directed 15 more projects related to computer vision and 3-D reconstructions from the Ministry of Science and Technology as well as industries in Taiwan. Her current research interests include 3-D reconstructions, computer vision, and augmented reality and related applications.

SHINFENG D. LIN (M'98–SM'17) received the Ph.D. degree in electrical engineering from Mississippi State University, in 1991. He was the Director of the Bureau of Education, Hualien County, Taiwan, from 2002 to 2003. He is currently a Professor with the Department of Computer Science and Information Engineering, National Dong Hwa University, Taiwan. He is also the Dean of Academic Affairs with National Dong Hwa University. His research interests include signal/image processing, pattern recognition, and information security. He is a Fellow of IET. He received the Gold Medal Award from the 2005 International Trade Fair ''Ideas-Inventions-New Products'' (IENA), Nuremberg, Germany.

RO-MIN WENG (M'08) received the Ph.D. degree in electrical engineering from National Taiwan University, Taipei, in 1999. She was the Chair of the Department of Electrical Engineering, National Dong Hwa University, Hualien, Taiwan, from 2010 to 2016. She was the Dean of Research and Development, from 2016 to 2018. Since 2011, she has been a Professor of the Department of Electrical Engineering, National Dong Hwa University. She has been the Chair of the Donghwa Innovation and Research Park, since 2018. Her research topics include wireless communication circuit design, mixed-signal circuit design, RF integrated circuit design, and video coding.

CHUAN-YU CHANG received the M.S. degree in electrical engineering from National Taiwan Ocean University, Keelung, Taiwan, in 1995, and the Ph.D. degree in electrical engineering from National Cheng Kung University, Tainan, Taiwan, in 2000. From 2001 to 2002, he was with the Department of Computer Science and Information Engineering, Shu-Te University, Kaohsiung, Taiwan. From 2002 to 2006, he was with the Department of Electronic Engineering, National Yunlin University of Science and Technology, Yunlin, Taiwan, where he has been with the Department of Computer and Communication Engineering (later Department of Computer Science and Information Engineering), since 2007, and is currently a Full Professor and the Dean of Research and Development. His current research interests include neural networks and their application to medical image processing, wafer defect inspection, digital watermarking, and pattern recognition. In the above areas, he has authored or coauthored more than 150 publications in journals and conference proceedings. He is the Chair of the IEEE Signal Processing Society Tainan Chapter and an Associate Editor of the *International Journal of Control Theory and Applications*.